Synthesis and behaviour of PEG-b-PDEAm block copolymers in aqueous solution

Xuewei Zhang, Tobias Burton, Martin In, Sylvie Begu, Anne Aubert-Pouëssel, Jean-Jacques Robin, Sophie Monge, Olivia Giani

Synthesis and behaviour of PEG-*b*-PDEAm Block Copolymers in Aqueous Solution

Xuewei Zhang,[1] Tobias F. Burton,[1] Martin In,[2] Sylvie Bégu, [1] Anne Aubert-Pouëssel, [1] Jean-Jacques Robin,[1] Sophie Monge,[1] Olivia Giani [1*]

[1] ICGM, Univ Montpellier, CNRS, ENSCM, Montpellier, France

[2] L2C, Univ Montpellier, CNRS, ENSCM, Montpellier, France

Correspondence to: Olivia Giani (E-mail: *olivia.giani@umontpellier.fr*)

ABSTRACT

Well-defined double hydrophilic block copolymers (DHBCs) of poly(ethylene glycol)-*block*-poly(N,N-diethylacrylamide) (PEG-*b*-PDEAm) were synthesized via a reversible addition-fragmentation chain-transfer (RAFT) polymerization of N,N-diethylacrylamide (DEAm) using dithioester terminated PEG of different chain lengths as macro-chain transfer agents. Controlled molecular weight and narrow molecular weight distribution were achieved as proven by size exclusion chromatography (SEC). Cloud points (CP) were determined via turbidity measurements with ultraviolet-visible spectroscopy (UV-vis) and LCST by differential scanning micro-calorimetry (micro-DSC). They range from 32 to 40°C depending on the PDEAm length block and its concentration. Above the LCST, fluorescence spectroscopy and dynamic light scattering (DLS) demonstrated that the PEG-*b*-PDEAm copolymers self-organized into large aggregates. More interestingly, copolymers pre-aggregated at relatively high concentrations below the LCST.

KEYWORDS: (N,N-diethylacrylamide, RAFT, thermosensitive polymers, behaviour in aqueous solution)

INTRODUCTION

Stimuli responsive double hydrophilic block copolymers (DHBCs) have attracted much interest due to their ability to form micelles in response to an external stimulus such as temperature, pH, salinity or a combination of different stimuli in aqueous solutions.[1-4] Consequently, such block copolymers display potential applications in the biomedical field as drug carrier systems,[4,5] biosensors,[6] biomimetic mineralization templates,[7-9] fluorescent chemosensors [10] as well as for gene therapy and in-vivo imaging/targeting.[11-12] Among the different possible structures, thermosensitive poly(ethyleneglycol)-*block*-poly(N-isopropylacrylamide) (PEG-*b*-PNIPAm) DHBCs were widely studied as they proved to be biocompatible.[1, 13-15] Above the lower critical solution temperature (LCST) and in aqueous solutions, such derivatives self-organize into micelles with the more hydrophobic PNIPAm block as the micelle core and the PEG block acting as the corona. Nevertheless, the development of PNIPAm based copolymers in medicine fields was limited due to the toxicity of N-isopropylacrylamide (NIPAm) monomer[16] (A). N,N-diethylacrylamide (DEAm) has the advantage of being a liquid which it more easier to use than NIPAM. As NIPAM has a secondary amide group it can be a proton acceptor and a donor acceptor, DEAm has a tertiary amide group ant it can only act as hydrogen bond acceptor. As DEAm is a less harmful monomer with similar LCSTs (32°C) when polymerized[17] and as the PDEAm has a lower cytotoxicity [16,18-20] (A, B,C) , the application of this monomer in polymers drugs becomes more practical. However, the LCST of PDEAm is not high enough for biomedical applications since the physiological temperature is around 37°C.

Copolymerization with a hydrophilic monomer can control phase transition behaviour. When N-vinylpyrrolidone is used as comonomer the LCST improves until 36°C when the copolymers are synthesised by a RAFT process using a trithiocodecanoic acid-2-cyanoisopropyl as RAFT agent and until 37,6 °C when synthesized by UV initiated polymerization process [21,22] (D ref Ngadaonye et E polymer 9) It is known that polymer topology affects LCST values. It is known that polymer topology affects LCST values. Wihttaker [23], in the case of PNIPAM showed that the star polymers had a lower LCST than linear polymers. Considering these factors PEG-*b*-PDEAm block copolymers should be an interesting DHBC to study. Indeed, for biomedical and pharmaceutical applications, PEG is a perfect hydrophilic polymer . It is known for its non-toxicity, biocompatibility properties and its resistance to recognition by the immune system. For example the synthesis of pegylated poly(N,N-diethylacrylamide) (PDEAm) block copolymers via reversible addition-fragmentation chain transfer (RAFT) polymerization from a trithiocarbonate chain transfer agent were performed in aqueous dispersion polymerization process.[24,25] To achieve that, a trithiocarbonate type chain transfer agent (CTA) was priorly bonded to poly(ethylene glycol) monomethyl ether by esterification to yield a PEG RAFT macro-CTA according to the well-known macroinitiator route.[26] Others pathways can also be used to afford block polymers. Three routes can be considered: (1) sequential living polymerization of two or more monomers [27] , (2) coupling of two or more homopolymers through chemical reaction such as " click chemistry" [28] or (3) end modification of a homopolymer to initiate another polymerization [29,30]; we report herein the synthesis of double hydrophilic PEG-*b*-PDEAm block copolymers using the last strategy. RAFT polymerization of N, N-diethylacrylamide was achieved using a dithioester-terminated PEG as a chain transfer agent preliminary prepared by end group modification of poly(ethylene glycol) monomethyl ether. The thermal behavior of copolymers was studied in order to evaluate the effect of the PEG and PDEAM blocks chain length on the LCST in water. The thermal aggregation behaviour of PEG-*b*-PDEAm in aqueous solution was also investigated using different analytic techniques, such as UV-visible spectroscopy (UV-Vis), differential scanning micro-calorimetry (micro-DSC), dynamic light scattering (DLS) and fluorescence spectroscopy.

EXPERIMENTAL

Materials

Monomethylether poly(ethylene glycol) with different molar masses (750, 1900, and 5000 g mol^{-1}) and N,N-diethylacrylamide were purchased from Polyscience Chemical Ltd. Maleic anhydride and all deuterium solvents were purchased from Sigma-Aldrich. Dithiobenzoic acid (DTBA) was prepared according to the process reported in the literature.[31] 1,4-Dioxane was distilled over calcium hydride under vacuum. Azobis-isobutyronitrile (AIBN) was recrystallized twice in ethanol. All other chemicals were used without further purification.

Preparation of poly(ethylene glycol) macro-chain transfer agent

The poly(ethylene glycol) macro-chain transfer agent was synthesized according to literature data.[13] In a typical experiment, poly(ethylene glycol) monomethyl ether (1900 g mol^{-1}, 4.75 g, 2.5 mmol) was dissolved in 50 ml of anhydrous toluene. Maleic anhydride (2.45 g, 25 mmol) was then added and the mixture was stirred at 75 °C for 24 hours. The resulting polymer was precipitated three times in large volumes of diethyl ether. Once filtered and dried, 4.8 g of white powder (PEG-MAh) was obtained (yield: 96%). ^{1}H-NMR (300 MHz, $CDCl_3$, δ, ppm): 3.35 (m, 3H, CH_3O-); 3.5-3.75 (s, CH_2); 4.35 (m, -CH_2COO-, 2H) and 6.2-6.5 (m, -COOCH=CH-, 2H).

In the next step, freshly prepared DTBA (3.2 g, 20.8 mmol) was added dropwise to a 50 ml solution of PEG-MAh (4.0 g, 2.0 mmol) in carbon tetrachloride under nitrogen. The mixture was then stirred at

70 °C for 20 hours. The resulting polymer was obtained after three precipitations in large volumes of diethyl ether. Once filtered and dried, 4.0 g of orange powder (PEG macro-CTA) was obtained (yield: 93%). ^{1}H-NMR (300 MHz, acetone d_6, δ, ppm): 3.35 (m, 3H, CH_3O-); 3.5-3.75 (s, CH_2); 4.35 (m, -CH_2COO-, 2H) and 7.45-8.1 (m, aromatic protons, 5H).

Synthesis of poly(ethylene glycol)-*block*-poly(N,N-diethylacrylamide) copolymers by RAFT polymerization

In a typical experiment, N,N-diethylacrylamide (5 g, 39 mmol), AIBN (0.02 g, 0.12 mmol), PEG macro-CTA (0.35 mmol), and 1,4-dioxane (14 mL) were introduced into a Schlenk tube under nitrogen. After three freeze-thaw cycles, the mixture was placed in a thermostated oil bath at 80 °C. Samples for the kinetic studies were taken under nitrogen at different intervals of the polymerization. The reaction was stopped by freezing the solution in liquid nitrogen. The residual PEG macro-CTA was eliminated by filtering the copolymer solution through a column of basic alumina gel using THF as eluent. ^{1}H-NMR (300 MHz, $CDCl_3$, δ, ppm): 1.0-1.5 (s, CH_3 of ethyl group in PDEAm block); 1.5-2.0 (s, CH_2 of acrylic group in PDEAm block); 2.2-2.8 (s, CH of acrylic group in PDEAm block); 2.95-3.5 (m, CH_2 of ethyl group in PDEAm block); 3.5-3.75 (s, CH_2 in PEG block) and 7.45-8.1 (m, aromatic protons, 5H).

Methods

Size exclusion chromatography (SEC) analysis was performed using a system equipped with PL Gel 500, 10^3, 10^4 columns (Polymer Laboratories company). THF was used as the eluent at a flow rate of 1.0 ml min^{-1}. Monodisperse polystyrene standards were used for the calibration curve.
The ^{1}H-NMR measurements were carried out on a Bruker AV-300 and AV-400 NMR spectrometers. Fourier transform infrared spectroscopy (FTIR) measurements were recorded with a PerkinElmer Spectrum 100 FT-IR spectrometer.
The cloud point measurements were performed on a PerkinElmer Lamba 35 UV-vis spectrometer. Temperature control of the samples was achieved using a PerkinElmer PTP1+1 Peltier with heating rates of 0.2 °C min^{-1} and measurement intervals of 0.1 °C at 500 nm. All PEG-*b*-PDEAm aqueous solution samples were prepared by dissolving 2 mg ml^{-1} of copolymer into deionized water at 15 °C then filtering through a 0.2 µm Millipore® nylon membrane. The LCST measurements were also performed by Differential Scanning Microcalorimetry using SETARAM Micro-DSC III 1 mL cells, in a range from -2 °C to 65 °C. Several heating and cooling cycles were performed at 0.1 °C min^{-1}. The LCST values were calculated at the endotherm's peak. The changes in solubility of aqueous solutions of copolymer versus temperature were performed by fluorescence spectroscopy with pyrene as a fluorescent probe. Steady-state fluorescence spectra were recorded on a Shimadzu RF-5301PC fluorescence spectro- meter at a 90° collection angle. Excitation spectra were monitored at 390 nm and emission spectra were monitored at 339 nm. Slit widths for both excitation and emission sides were maintained at 3.0 nm. Temperature control of the samples was achieved using a water-jacketed cell holder connected to a LAUDA circulating bath. Sample solutions were prepared by dissolving 10 µl of a 2 mmol l^{-1} pyrene in methanol solution into 10 ml of a PEG-*b*-PDEAm aqueous solution under stirring. Measurements of the size of the objects were performed using Dynamic Light Scattering (DLS) on a High Performance Zetasizer Nano instrument (Malvern, U.K.) with a wavelength of 633 nm and at a 173° scattering angle or with a Brookhaven BI-200SM Laser light scattering system with a digital correlator (BI-9000AT). The light source of the BI-200SM was a Uniphase 50mW Ar+- laser (λ = 514.5 nm). Measurements were carried out at a 90° scattering angle at different temperatures. The time autocorrelation functions were analyzed with CONTIN or CUMULANT methods.

RESULTS AND DISCUSSION

RAFT polymerization of DEAm with dithioester-terminated PEG

The reactional pathway for the synthesis of PEG-*b*-PDEAm block copolymers is shown in Scheme 1. An initial reaction between maleic anhydride and poly(ethylene glycol) monomethyl ether yielded a intermediate (PEG Mah) containing both vinyl and acid functions. This intermediate was then functionalised with dithiobenzoic acid to lead to the PEG macro-CTA.

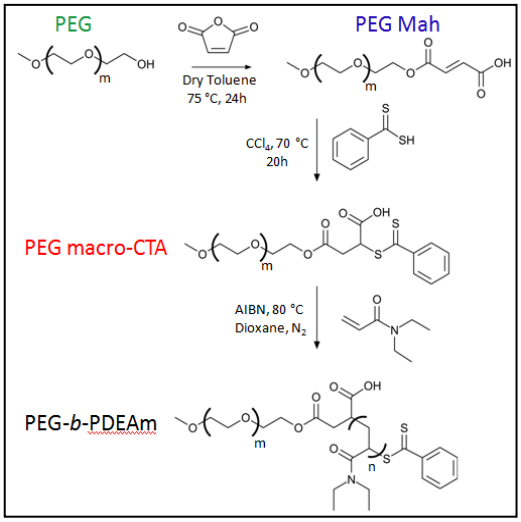

Scheme 1 Synthetic pathway for the PEG-*b*-PDEAm block copolymers.

Chemical structures of the intermediate and final PEG-*b*-PDEAm copolymers were confirmed by ^{1}H-NMR spectroscopy (Figure 1). The ^{1}H-NMR spectrum of the PEG macro-chain transfer agent (Figure 1, g) showed peaks at 7.45-8.1 ppm which were ascribed to the aromatic protons a" of the dithiobenzoate group and peaks at 5.3 and 3.1 ppm corresponding to the methine and the methyl groups close to the dithioester (d" and e" respectively). Furthermore, FT-IR spectroscopy (Figure 1, c) revealed bands appearing at 688, 764 and 1729 cm^{-1} which can be assigned respectively to the aromatic ring and the carbonyl from DTBA. The ^{1}H-NMR spectrum of the PEG-*b*-PDEAm copolymers (Figure 1, h) display peaks at 7.4-8.0 ppm and 3.6 ppm which were ascribed respectively to the aromatic protons a'''of the RAFT group and methyl protons f''' of the PEG block. The peaks of the PDEAm block were observed at 2.9-3.5 ppm, 0.9-1.5 ppm, 2.2-2.8 ppm and 1.5-2.0 ppm. Respectively, those peaks correspond to the methylene protons c''', methyl protons b''' of the diethyl groups, the methylene protons (see e''') and methine protons (see d''') of the polymer backbone. Furthermore, FTIR spectroscopy proved the presence of characteristic bands at 1103 and 1624 cm^{-1} corresponding respectively to the ether bond of the PEG block and the carbonyl groups of the PDEAm block.

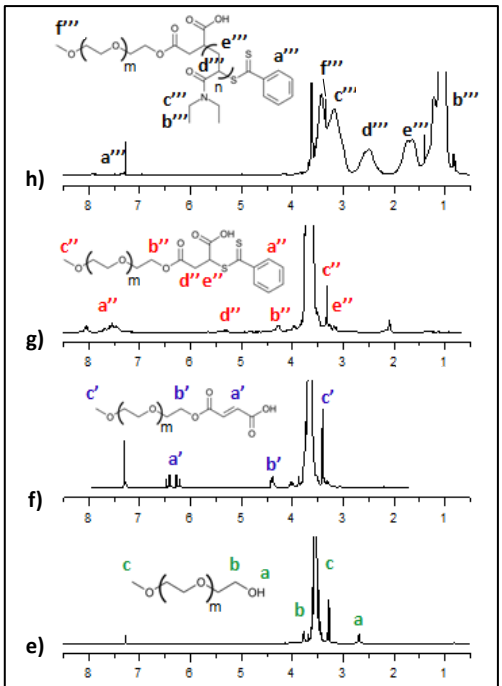

Figure 1 ^{1}H-NMR (300MHz, $CDCl_3$) and FT-IR spectra of PEG monomethyl ether (a and e); acid terminated PEG (b and f); PEG macro-CTA (c and g); PEG-*b*-PDEAm (d and h).

Table 1 Characterization data of PEG-*b*-PDEAm copolymers obtained via RAFT polymerization of DEAm using dithioester terminated PEG of various chain lengths as macro-CTAs: [Monomer]:[macro-CTA]:[AIBN]= 672:6:1.

Block copolymer[a]	M_n of PEG (g mol^{-1})[b]	Monomer Conversion (%)	$M_{n,th}$ of copolymer (g mol^{-1}) [c]	$M_{n,exp}$ of copolymer (g mol^{-1}) [d]	$Đ$
PEG_{16}-*b*-$PDEAm_{70}$ (**P1**)	750	63	9700	9645	1.10
PEG_{42}-*b*-$PDEAm_{77}$ (**P2**)	1900	63	10900	11700	1.10
PEG_{113}*b*-$PDEAm_{89}$ (**P3**)	5000	62	13900	16300	1.11

[a] Theorical degree of polymerization for PDEAm is equal to 78

[b] Mn of PEG used for the synthesis of the macroCTA

[c] $Mn,th = M_{macroCTA} + ([M]_0/[macroCTA]_0 \times M \text{ of monomer} \times \text{conversion})/100$.

[d] Estimated by SEC in THF with PS standards.

The RAFT polymerization of N, N-diethylacrylamide with PEG macro-CTA and AIBN in dioxane at 80 °C led to well defined PEG-*b*-PDEAm copolymers using the experimental conditions reported in a previous study.[32] (Table 1). Monomer conversions were determined by ^{1}H-NMR spectroscopy. As shown in figure 2 (top), the first-order kinetic plots were approximately linear. Moreover, the rate of polymerization was not affected by the chain length of the PEG macro-CTA used. An inhibition period was observed at the beginning of each polymerization with the largest PEG macro-CTA inducing the shortest inhibition period. Size exclusion chromatography demonstrated a linear evolution of molecular weights in respect to the monomer conversion (figure 2, bottom). Furthermore, the dispersity of the copolymers was narrow throughout the polymerization reactions ($Đ$ < 1.1). The linearity of these evolutions and low dispersities indicated that the concentration of radical species remained constant throughout the reaction and that termination reactions were not significant, proving a well controlled polymerization.

Size exclusion chromatography of the precipitated copolymers in diethyl ether showed the presence of some remaining PEG macro-CTA. (Figure 3) The simple precipitation of the final reaction mixture in diethyl ether did not efficiently purify the copolymers as it is the case usually for similar block copolymers.[33] This was attributed to the insolubility of the PEG macroCTAs in the solvent. Accordingly, we developed a purification method, which consisted of eluting a THF solution of the copolymer through a column of basic alumina. This method has proved to be efficient for the short PEG macro-CTAs (750 and 1900 g mol^{-1}) but not for the larger PEG macro-CTA (5000 g mol^{-1}). It is important to note that the samples taken during the reaction for kinetic study were also purified using this method.

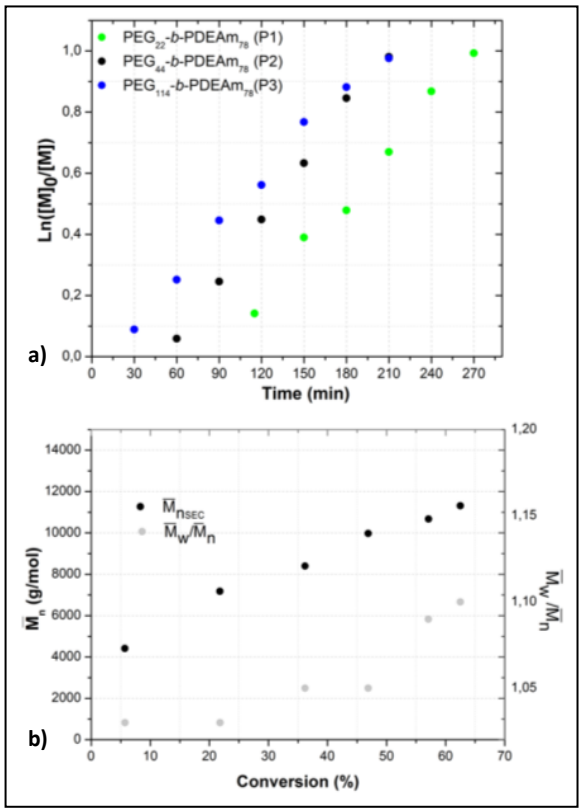

Figure 2 a) First-order kinetic plots of DEAm polymerizations with PEG macro-CTAs of different chain lengths (750 (**P1**), 1900 (**P2**) and 5000 (**P3**) g mol^{-1}) in dioxane at 80 °C. [Monomer]:[macro-CTA]:[AIBN]= 672:6:1. b) Evolution of Mn vs. monomer conversion for the polymerization of DEAm initiated by PEG_{44} macro-CTA 1900 g mol^{-1} (**P2**).

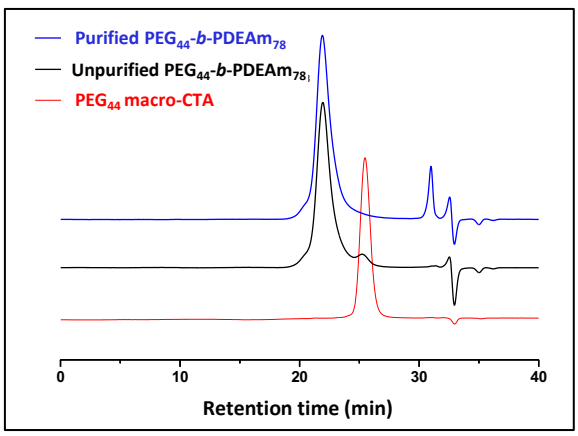

Figure 3 Chromatograms of PEG_{44} macro-CTA (red), non purified **P2** (black) and purified **P2** copolymers (blue).

Behaviour of PEG-*b*-PDEAm block copolymers in aqueous solution

Aqueous solutions of the copolymers showed a phase separation (demixion) when the temperature raised above the polymer's LCST.[34] This phase transition causes a change of turbidity as well as an endothermic phenomenon due to a disruption of hydrogen bonds within the solution. As stated previously, both PDEAm and PEG are thermosensitive polymers with LCSTs in aqueous solution of 32 °C and 100 °C, for PDEAm and PEG, respectively. [35-37] It is known that the LCST of block copolymers composed of two thermosensitive moieties lies in between the LCST values of its two blocks. This intermediary value can be tuned by adjusting the molar ratio of both blocks.[38] As a consequence, the LCST of PEG-*b*-PDEAm copolymers were expected to be higher than 32 °C. The phase transition temperature of aqueous solutions of the copolymers was measured by UV-vis spectroscopy and micro-DSC.

Determination of the CP by UV-Vis spectroscopy

The change of turbidity followed by UV-visible spectroscopy determined the cloud point (CP). Figure 4 illustrates the evolution of the UV-Vis transmittance of aqueous solutions of homopolymer and copolymers at 0.2 % (w/v) when heated. It is characterized by a sudden and sharp decrease of the transmittance from close to 100% to close to 0%. The CP values were taken at 50% transmittance at 500 nm. As expected, the CPs of the copolymers were higher than that of the homopolymer. These CPs were measured at 33, 35, 35, and 36 °C for PDEAm, **P1**, **P2**, and **P3** respectively. The CP values were similar for **P1** and **P2** due to the small difference of composition whereas the CP for **P3** was superior as the amount of PEG as significantly larger. The hydrophilic nature of the PEG block promoted the hydration of the copolymer for higher PEG molar masses, which in turn, increased the CP value. Moreover, the decrease of the cloud point could be explained by the fact that the thermosensibility of the copolymer is principally related to the PDEAm block in the copolymer. The PDEAm block represents 92 %wt of **P1**, 84 %wt of **P2** and 69 %wt of **P3**. This variation in PDEAm content could explain the decrease of the cloud point when the content of the PDEAm block is greater.

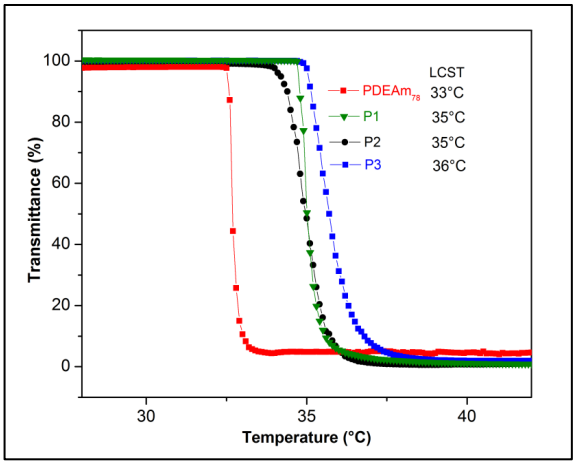

Figure 4 Transmittance (%) of solutions of PDEAm (red), **P1** (green), **P2** (black) and **P3** (blue) in 0.2 % (w/v) in respect to temperatures (0.2 °C min^{-1}).

The effect of the concentration on the CP of aqueous solutions of **P2** was also investigated (Figure 5). The CP diminished with the increase of concentration in relatively dilute solutions (<1 %), whereas no significant effects were observed when the concentration exceeded 1 %.

The initial value of the transmittance depends on the concentration. The phase transition, as demonstrated by Osváth et al. on Poly NIPAM, is broad at high dilution (0.02 %).[39] When the concentration increases, the transitions become narrow and shift towards lower temperatures. The cloud point decreases with increasing polymer concentrations to become identical to that of PDEAm. A concentrated solution of 10 % presented a lower initial transmittance due to aggregation phenomena. The 0.1 % solution demonstrated a singular behaviour as the transmittance rose again after decreasing; this was attributed to aggregates sedimentation.

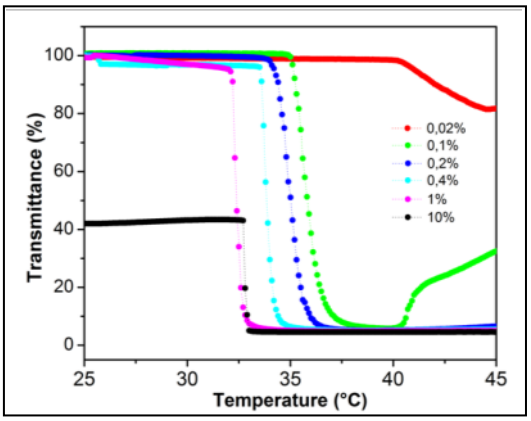

Figure 5 Effect of the concentration on the CP of aqueous solutions of **P2** measured by UV-Vis (heating rate: 0.2 °C min^{-1}).

The LCSTs of aqueous solutions of **P2** and **P3** at 10 % (v/w) were also determined by micro-DSC with a 0.1 °C min^{-1} heating rate (see supporting information). The LCST values were higher than those obtained by UV-vis: 36.8 and 37.3 °C for **P2** and **P3** respectively. These slight differences can be explained by the differences between the analytical techniques. In the examined temperature range, the phase transition of the PEG block could not be detected and the variations in the heat flow were due to the disruption of hydrogen bonds in the various PDEAm blocks in **P2** and **P3** (84 % wt and 69 % wt respectively). [40]

Behaviour of PEG-*b*-PDEAm copolymers in solution

The effect of the temperature on the solubility of these copolymers in aqueous solutions was monitored by fluorescence spectroscopy using pyrene, a well-known polarity-sensitive probe, as the fluorescent probe. Pyrene is a strongly hydrophobic aromatic molecule and its solubility in water is

very low. Therefore, pyrene is preferentially located inside hydrophobic regions such as those found inside self-assembled object. Emission spectra of pyrene (2 10^{-6} M) in a 1 % (w/v) aqueous solution of polymer were recorded at various temperatures for **P2** and **P3**. The intensity ratio between the first (I_1, λ = 373nm) and third (I_3, λ = 393nm) highest energy emission peaks, known as the I_1/I_3 ratio, was used as an indicator of the chromophore's local environment.[41] The I_1/I_3 ratios of pyrene from emission spectra of **P2** and **P3** are plotted in figure 6 (star and circle plots).

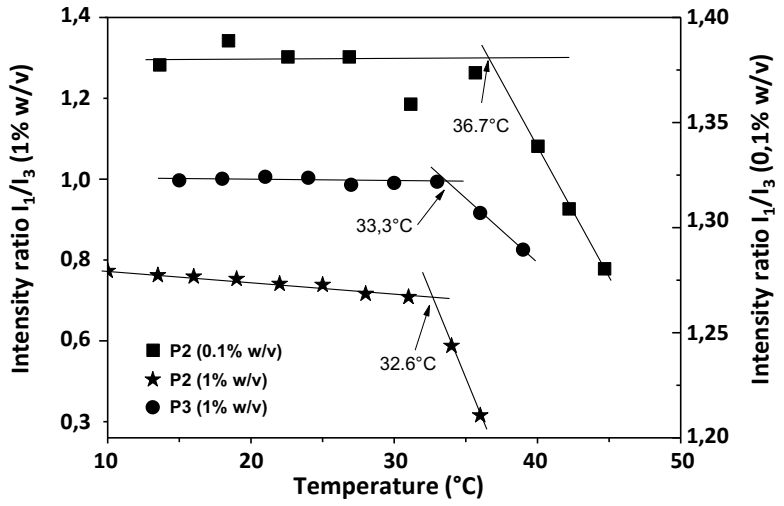

Figure 6 Temperature dependence of the fluorescence intensity ratio I_1/I_3. **P2** (0.1% w/v) (square); **P2** (1% w/v) (star) and **P3** (1% w/v) (circle). [Pyrene] = 2 10^{-6}M.

It can be observed that the initial I_1/I_3 ratios are different for **P2** and **P3** and are relatively low. The I_1/I_3 ratio of pyrene in water is approximately 1.9 whereas in this study, the initial I_1/I_3 ratios for **P2** and **P3** are 0.8 and 1 respectively with concentrations of 1 %wt. The fluorescence of pyrene quantified by ratios I_1/I_3 and I_{337}/I_{334} depends on the polar environment. The relatively low value for **P2** (1% w/v) when compared to that of **P3** could possibly be due to attractive interactions between pyrene and PDEAM blocks. This hypothesis is suggested by the decrease of this ratio when the composition of DEAM moieties increases in the copolymer. Indeed, the proportion of the PDEAm block is greater in **P2** than in **P3** (84 % vs 69 % respectively). The same phenomenon explains the increase of the ratio when the concentration is lowered (0,1% w/v), suggesting the formation of more hydrophobic micro-domains. The sudden decrease of I_1/I_3 ratios at increasing temperatures showed that the molecules of pyrene were transferred from water into a nonpolar environment. A decrease of the I_1/I_3 ratio was observed below the demixing temperature of **P2** which indicated a change in the probe's microenvironment as reported elsewhere.[42] Water may start to behave as a selective solvent for PEG blocks meaning a lower quality of solvent for the PDEAm chains.

The transition temperature of **P3** was observed to be higher than that of **P2**, which was in accordance with the CP values of the copolymer measured by UV-vis. The temperature of transition of **P2** copolymers in solution decreased when increasing the concentration. The same concentration effects were observed in aqueous solutions of homologous PEG-*b*-PNIPAm copolymers.[40]

Determination of aggregate size

Dynamic light scattering (DLS) was used to examine the dynamics of concentration fluctuations which is related to the size of the macromolecules but also to their interactions: large polymer diffuse more slowly so that the fluctuations of concentration relax more slowly. The diffusion coefficient decreases with concentration for attractive macromolecules. When the polymers attract each other they diffuse more and more slowly when the concentration increases and very wide apparent hydrodynamic radius are measured.[43]

The hydrodynamic diameter (D_h) values of these macromolecular chains (see supporting information) at different concentrations (from 0.01 % to 10 % w/v) were determined by dynamic light scattering (DLS) measurements at 20 °C. When the concentration increases from 0.1 % to 10 %, the particle sizes are identical for P2 and P3 around 7 nm. At temperatures lower than the LCST, water is a theta solvent for the copolymers at 20°C and the chains are probably Gaussian.

The intensity of light scattered during a heating/cooling cycle is plotted as a function of temperature for a solution at 0.1 % w/v of **P2** (Figure 7). The mean photon count rate slowly rose between 16 and 32.9 °C (region I), then rapid increases occurred between 32.9 °C and 36.8 °C (regions II). A decrease in the mean photon count rate then occurred at 36.8 °C (region III).

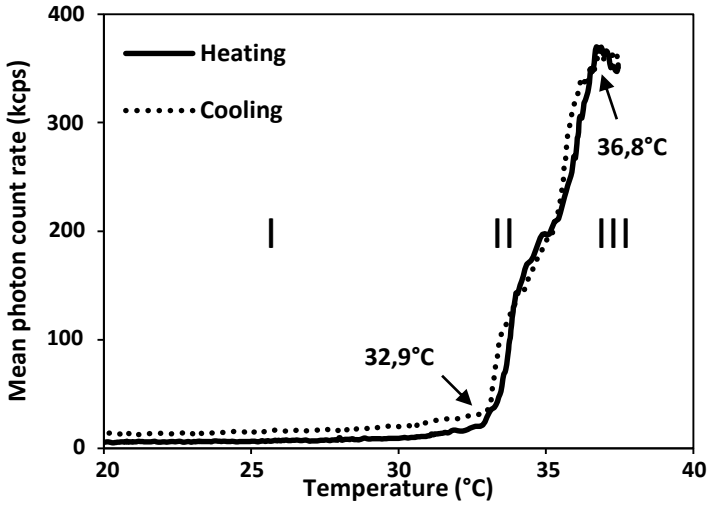

Figure 7 Plot of the mean photon count rate of a 0.1 % w/v solution of **P2** vs. temperature (heating/cooling rates = 0.2 °C min^{-1}).

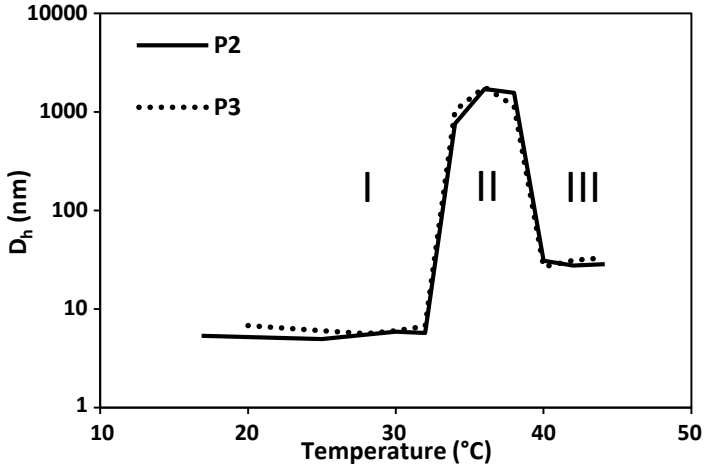

Figure 8 Influence of the temperature on the hydrodynamic diameters of **P2** and **P3** in 0.1 % (w/v) solutions.

In solution, the variation of the scattered light intensity can be explained by an increase of the molar mass of the objects in solution or an increase of the attractive interactions resulting in a second virial coefficient getting more and more negative. Hence, the slow increase of the scattered light intensity at low temperature can be explain from a variation of the attractive interactions. At 32.9°C, the macromolecules start to aggregate which result in a jump in the scattered light intensity.[43] This rise in scattered intensity is associated with a slowing down of the dynamics of concentration fluctuation of concentration, which characteristic time has been translated in terms of hydrodynamic radius in figure 8. The changes in hydrodynamic diameters of **P2** and **P3** in solution versus temperature are consistent with the results of the mean photon count rate of figure 7, but the sizes associated are huge and suggest a demixing rather than a micellization process.

The aggregate size distribution was also measured at different temperatures (Figure 9). At 20°C two populations are observed: the small one at 7nm and a large one at 400nm. This is typical for polymers not in good solvent. Increasing the temperature up to 30°C broadens the distribution of large size, with a new mode appearing at 100 nm. Note that the proportion of the large particles increases, this reveals a decrease in the quality of the solvent as temperature increases. Upon further increase of the temperature, beyond 34°C, the small size population is no longer observed, only large particles are observed which size stabilize at 2000nm at the highest temperature, meaning that the copolymers are in bad solvent above 34°C. (Note that the large size presented have no meaning but just reflects the slowing down of the fluctuations of concentration due to attraction betwen macromolecules). Indeed, the pre-aggregation phenomena of PDEAm chains at temperatures below the LCST was already described and reported in the literature which confirmed our experimental results.[44] The size of the aggregates increased when heated. When the temperature approached and exceeded the LCST, the size distribution of aggregates became monodisperse and narrow.

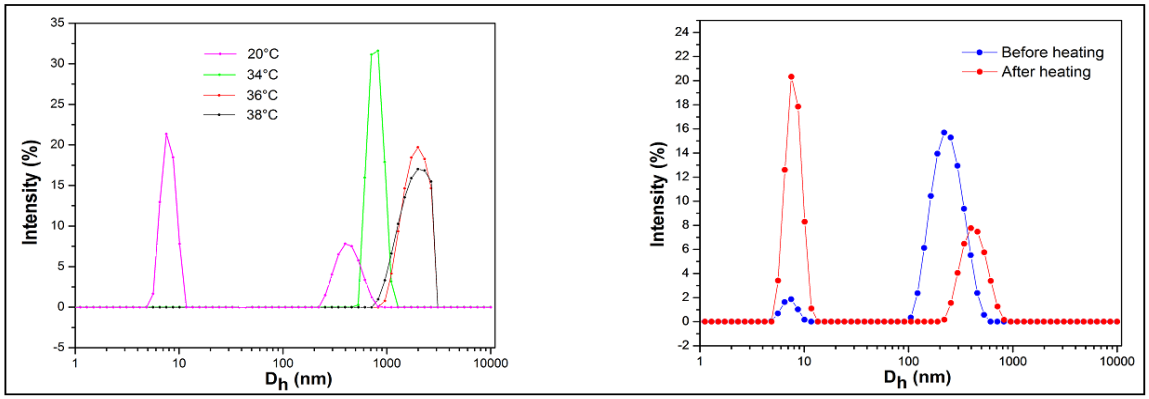

Figure 9 Size distribution of **P2** in a 0.1% (w/v) solution at different temperatures (Left) and at 20 °C before and after heat treatment (Right).

CONCLUSIONS

Well-defined PEG-*b*-PDEAm block copolymers were successfully synthesized via RAFT polymerization using a dithioester-terminated PEG as a macro-CTA with different chain lengths. The polymerization kinetics were investigated and demonstrated that the polymerization was controlled. An inhibition period was observed at the beginning of all polymerizations initiated by different chain lengths of macro-CTA. The largest macro-CTA induced the shortest inhibition period. Once the copolymers were prepared, the LCSTs of these copolymers were determined in aqueous solutions of different concentrations by UV-Vis and micro-DSC. These CP values were observed in the range of 32-40 °C and depended on the wt% of PDEAm block chain length in the copolymer. The thermal aggregation behaviour was also investigated by fluorescence spectroscopy and DLS. The results of these measurements revealed a pre-aggregation of polymers in aqueous solution below the LCST. Above the LCST the size of aggregates improves causing an increase of the turbidity of the solution.

REFERENCES AND NOTES

1. J. Virtanen, H. Tenhu, Macromol. 33 (2000) 5970-5975.
2. S. Liu, J. V. M Weaver, M. Save, S. P. Armes, Langmuir 18 (2002) 8350-8357.
3. L. Gu, C. Feng, D. Yang, Y. Li, J. Hu, G. Lu, X. Huang, J. Polym. Sci., Part A: Polym. Chem. 47 (2009) 3142-3153.
4. C. Chen, T. H. Kim, W. Wu, C. Huang, H. Wei, C. W. Mount, Y. Tian, S. Jang, S. H. Pun, A. K. Y. Jen, Biomaterials 34 **(**2013) 4501-4509.
5. S. Wang, Y. Yang, Y. Wang, M. Chen, Int. J. Pharm. 495 (2015) 840–848.
6. Q. Cai, K. Zeng, C. Ruan, T. A. Desai, Grimes, C. A., Anal. Chem. 76 (2004) 4038-4043.
7. X. Yao, H. Yao, G. Li, Y. Li, J. Mater. Sci. 45 (2010) 1930-1936.
8. E. Molina, J. Warnant, M. Mathonnat, M. Bathfield, M. In, D. Laurencin, C. Jérôme, P. Lacroix-Desmazes, N. Marcotte, C. Gérardin, Langmuir 31 (2015) 12839-12844.
9. J. Reboul, T. Nugay, N. Anik, H. Cottet, V. Ponsinet, M. In, P. Lacroix-Desmazes, C. Gerardin, Soft Matter 7 (2011) 5836-5846.
10. J. Han, B. An, Y. Wang, X. Bao, L. Ni, C. Li, L. Wang, X. Xie, Sens. Actuator B-Chem. 250 (2017) 436-445.
11. A. V. Kabanova, V. A. Kabanov, Adv. Drug Deliv. Rev. 30 (1998) 49–60.
12. T. H. Kim, C. W. Mount, B. W. Dulken, J. Ramos, C. J. Fu, H. A. Khant, W. Chiu, W. R. Gombotz, S. H. Pun, Mol. Pharm. 9 (2012) 135−143.

13. W. Zhang, L. Shi, K. Wu, Y. An, Macromol. 38 (2005) 5743-5747.
14. M. D. C. Topp, P. J. Dijkstra, H. Talsma, J. Feijen, Macromol. 30 (1997) 8518-8520.
15. C. Y. Hong, Y. Z. You, C. Y. Pan, J. Polym. Sci., Part A: Polym. Chem. 42 (2004) 4873-4881.
16. M.A. Coopertsein, H.E.Canavan, Biointerphases 8 (2013), 19.
17. A. Gandhi, A. Paul, S. Oommen Sen, K. Kumar Sen, Asian J. Pharma. Sci. 10 (2015) 99-107.
18. M. Panayiotou, C. Pöhner, C. Vandevyver, C. Wandrey, F. Hilbrig, R. Freitag, React. Fund. Polym. 67 (2007) 807-819.
19. X. Zhang, Z. Yang, D. Xie, D. Liu, Z. Chen, K. Li, Z. Li, B. Tichnell, Z. Liu, Designed monomers and Polymers 21 (2018), 43-54.
20. R.H. Perera, H. Wu, P. Peiris, C. Hernandez, A. Burke, H. Zhang, A. A. Exner, Nanomed. 13 (2017) 59-67.
21. J. I. Ngadaonye, L.M. Geever, M.O. Cloonan, C. L. Higginbotham, J. Polym. Res. 19 (2012) 9822-9837.
22. Y.S. Huang, J.K. Chen, T. Chao, C.F. Huang, Polymer 9 (2017) 231-245.
23. R. Plummer, D.J.T. Hill, A.K. Whittaker, Macromol. 39 (2006) 8379-8388.
24. J. Rieger, C. Grazon, B. Charleux, D. Alaimo, C. Jerôme J. Polym. Sci., Part A: Polym. Chem. 47 (2009) 2373-2390.
25. C. Gazon, J. Rieger, N. sanson, B. Charleux, Soft Matter 7 (2011) 3482-2490.
26. D. J. Keddie, Chem. Soc. Rev. 43 (2014) 496-505.
27. S. Sugihara, K. Hashimoto, S. Okabe, M. Shibayama, S. Kanaoka, S. Aoshima, Macromol. 37 (2004) 336-343.
28. R.A. Evans, Aust. J. Chem. 60 (2007) 384-395.
29. J.M. Rathfon, G.N. Tew, 49 (2008) 1761-1769.
30. S. Monge, O. Giani, E. Ruiz, M. Cavalier, J.J. Robin, Macromol. Rapid. Comm. 28 (2007) 2272-2276.
31. F. Becke, H. Hagen (BASF AG). German Patent 1 274 121, 1968.
32. X. Zhang, O. Giani, S. Monge, J. J. Robin, Polymer 51 (2010) 2947-2953.
33. Y. Ren, X. Jiang, J. Yin, Eur. Polym. J. 44 (2008) 4108-4114.
34. S. Ito, Kobunshi Ronbunshu 46 (1989) 437-43.
35. I. Idziak, D. Avoce, D. Lessard, D. Gravel, X. X. Zhu, Macromol. 32 (1999) 1260-1263.
36. S. Bekiranov, R. Bruinsma, P. Pincus, Phys. Rev. E. 55 (1997) 577.
37. R. L. Cook, H. E. King, D. G. Peiffer, Phys. Rev. Lett. 69 (1992) 3072
38. H. Y. Liu, X. X. Zhu, Polymer 40 (1999) 6985-6990.
39. Z. Osváth, B. Iván, Macromol. Chem. Phys. 218 (2017) 16400470
40. Y. Xia, N. A. D. Burke, H. D. H. Stover, Macromol. 39 (2006) 2275-2283.
41. K. Kalyanasundaram, J. K. Thomas, J. Am. Chem. Soc. 99 (2002) 2039-2044.
42. R. Motokawa; K. Morishita, S. Koizumi, T. Nakahira M. Annaka, Macromol. 38 (2005) 5748-5760.
43. M. Schärtl, In Light Scattering from Polymer Solutions and Nanoparticle Dispersions; Springer-Verlag Berlin Heidelberg 2007; J. Gao, C. Wu, Macromol. 30 (1997) 6873-6876.
44. Q. Cui, F. Wu, E. Wang, J. Phys. Chem. B 115 (2011) 5913-5922.